

On the Diffusion Impedance at Semiconductor Electrodes

Z. Hens[†] and W. P. Gomes*

Laboratorium voor Fysische Chemie, Universiteit Gent, Krijgslaan 281, B-9000 Gent, Belgium

Received: January 22, 1997; In Final Form: April 7, 1997[®]

It is well known that at metal electrodes, mass transport limitations introduce a Warburg impedance in the electrochemical impedance of an electrode process. Semiconductor electrodes, however, react differently from metal electrodes to variations of the applied potential, so that the influence of diffusion on the electrochemical impedance is less straightforward. In this paper, we propose a general approach of this problem, allowing to describe both the metal and semiconductor electrode behavior by using appropriate kinetical models. When discussing the diffusion impedance at ideal semiconductor/electrolyte contacts, distinction must be made between direct capture reactions and direct injection reactions. Whereas the former result in a Randles-like equivalent circuit, no Warburg component is present in the impedance spectrum of the latter if the reverse reaction is negligible. Thus, the electrochemical impedance provides a clear distinction between both reaction types. At nonideal semiconductor/electrolyte contacts, the situation is different because of the unpinning of the band edges. This may result in a Warburg impedance appearing in the electrochemical impedance of an injection reaction as well, i.e. if the shift of the band edges influences the rate constant of the injection reaction.

1. Introduction

Transport of dissolved electroactive species between the bulk solution and the electrode/electrolyte interface is a basic aspect of an overall electrode process. Therefore, this diffusion process¹ should have an influence on the electrochemical impedance of the electrode reaction, as far as it is affected by a perturbation of the potential across the electrode/electrolyte interface.

At metal electrodes, any change in the applied potential will produce a corresponding potential drop across the Helmholtz layer,^{3,4} thus affecting the rate constants of the charge-transfer reactions. On the basis of the Butler–Volmer equation to describe the kinetics of the electrode process, Randles showed that for a simple 1 equiv charge-transfer reaction, the mass transport appears in the electrochemical impedance as a Warburg impedance in series with the charge-transfer resistance.⁵ This impedance, being proportional to $1/(i\omega)^{1/2}$ (ω = pulsation), appears in the Nyquist plane characteristically as a line with a slope of -1 .

At semiconductor electrodes, distinction should be made between ideal and nonideal semiconductor/electrolyte contacts. An ideal semiconductor/electrolyte contact is characterized by the fact that, under depletion conditions, a variation of the applied potential will cause an equal change of the potential drop across the space–charge layer in the semiconductor.^{4,6,7} Therefore, the rate constants⁸ of the electrode reactions are not affected by potential variations, thus invalidating the use of the Randles model for these electrodes. On the contrary, the potential drop across the Helmholtz layer will change upon applying a potential variation to a nonideal semiconductor/electrolyte contact. In this case, the rate constants of the electrode reactions are effectively changed.⁷

In this paper, we present a procedure for modeling the mass transport which can be applied to both metal and semiconductor electrodes. We will start with a general description of the

diffusion process between the bulk electrolyte and the electrode/electrolyte interface. Combining the result with the Butler–Volmer equation yields the impedance at metal electrodes already mentioned. Next, we describe two types of simple one-step reactions at dark semiconductor electrodes, using well-known expressions for their kinetics. At an ideal dark semiconductor/electrolyte interface, direct capture processes, i.e. capture of majority charge carriers by electroactive species in solution, yield an electrochemical impedance formally equivalent to the Randles circuit. In contrast, no Warburg impedance is observed during injection reactions, i.e. either electron injection by reducing agents or hole injection by oxidizing agents in solution, if the rate of the reverse reaction is negligible. This difference allows one to distinguish between both processes by means of impedance measurements. We will further discuss nonideal semiconductor/electrolyte contacts, at which the situation is complicated by the varying potential drop across the Helmholtz layer. This leads to variations of the rate constants of the electrode reactions, thus introducing a Warburg impedance into the electrochemical impedance of injection reactions as well. Finally, these different cases will be illustrated by experimental results, obtained both at GaAs and InP electrodes.

2. Theoretical Description of the Mass Transport in an Overall Electrode Process

2.1. General Description. During an electrochemical process, electroactive species are consumed and produced at the electrode/electrolyte interface. This brings about gradients in the concentrations of these species near the interface, thus creating a driving force for mass transport by diffusion. The combination of mass transport and electrode reaction may be described by Fick's second law, imposing the appropriate boundary conditions.

For every electroactive species S (concentration c (m^{-3})), there exists at the interface a balance between the reaction rate (R ($\text{m}^{-2} \text{s}^{-1}$)), the local production rate (G ($\text{m}^{-2} \text{s}^{-1}$), i.e. generation caused by the reaction of other species at the interface), and the supply or removal by diffusion (J ($\text{m}^{-2} \text{s}^{-1}$)). A continuity equation for species S , written for a volume

[†] Research assistant of the FWO-Vlaanderen (Fund for Scientific Research–Flanders (Belgium)).

[®] Abstract published in *Advance ACS Abstracts*, July 1, 1997.

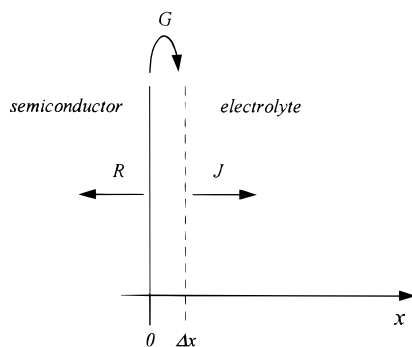


Figure 1. Illustration of the continuity equation at the electrode/electrolyte interface, in terms of reaction rate (R), diffusion flux (J), and local generation rate (G). The diffusion flux is considered positive in the direction indicated.

element of electrolyte with thickness Δx and unit area, describes this situation near the interface. Situating the interface at position $x = 0$ while stretching the volume element out between 0 and Δx (see Figure 1), the continuity equation becomes

$$\frac{dc^S}{dt}|_{x=0} \Delta x = G^S|_{x=0} - J^S|_{x=\Delta x} - R^S|_{x=0} \quad (1)$$

Taking the limit $\Delta x \rightarrow 0$ yields an equation which acts as a boundary condition at the interface for the diffusion of the species S between the bulk of the electrolyte and the interface:

$$G^S|_{x=0} = J^S|_{x=0} + R^S|_{x=0} \quad (2)$$

Assume now all rates consist of a time-independent bias and a small, time-dependent perturbation (indicated by an asterisk). Since the bias rates themselves obey (2), the perturbations are related by the same equation. Dropping the species indication, we get

$$G^*|_{x=0} = J^*|_{x=0} + R^*|_{x=0} \quad (3)$$

The mass transport term in this equation (J^*) may be calculated explicitly applying Fick's second law with the concentration of the species S at the interface ($c(0)$) as a parameter and the constant concentration of the species in the bulk as a boundary condition (cf. Appendix A or refs 2 and 9). For a sinusoidal perturbation with frequency $\omega/2\pi$ (generally written as $a^* = \tilde{a} \exp(i\omega t)$), this results in the following expression:

$$\tilde{J}|_{x=0} = \sqrt{i\omega D} \coth\left(\sqrt{\frac{i\omega}{D}} \delta\right) \tilde{c}(0) \quad (4)$$

In this formula, D stands for the diffusion coefficient of species S , while δ is the thickness of the diffusion layer. For ease of use, we define $d(\omega)$ as

$$d(\omega) = \sqrt{i\omega D} \coth\left(\sqrt{\frac{i\omega}{D}} \delta\right) \quad (5)$$

If the ratio $\omega\delta/D$ is sufficiently large, $d(\omega)$ reduces to $(i\omega D)^{1/2}$, which is proportional to the inverse of the Warburg impedance. It is indeed (4) that will account for this component appearing in the electrochemical impedance of many diffusion-limited electrode processes. Anticipating this result, we will refer to $d(\omega)^{-1}$ as the diffusion impedance. Figure 2 represents a Nyquist plot¹⁰ of $d(\omega)^{-1}$, calculated assuming $\delta = D = 1$.

Combining (5), (4), and (3) results in an equation which couples the mass transport to the electrode reaction by

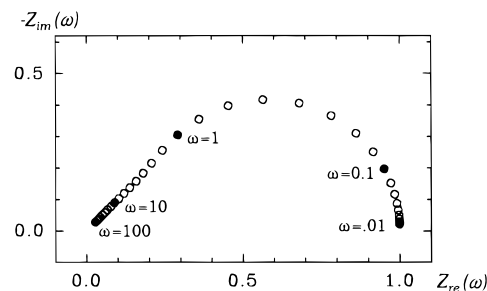


Figure 2. Nyquist representation of the diffusion impedance $d(\omega)^{-1}$ calculated assuming $D = \delta = 1$.

means of the concentration of the electroactive species at the interface:

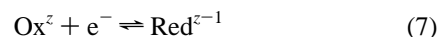
$$\tilde{G}|_{x=0} = \tilde{R}|_{x=0} + d(\omega) \tilde{c}(0) \quad (6)$$

This equation may act as a starting point to include the contribution of mass transport to the electrochemical impedance of the overall electrode process for metal electrodes as well as for semiconductor electrodes. In a general way, (6) shows that the mass transport will appear in the electrochemical impedance of the electrode process only if the concentration of the electroactive species near the interface is modulated by the varying electrode potential. If $\tilde{c}(0) = 0$, the term in $d(\omega)$ drops out, thus eliminating the part of the mass transport in the dynamic equations describing the electrode process.

The modulation of the concentration of the electroactive species at the interface will be realized if the reaction rate of this species is potential-dependent. Indeed, a variation of the electrode potential will then cause a more or less intense consumption of the species, thus modulating its concentration.

To make this analysis more detailed, a coupling between this equation and the applied potential perturbation must be made. This is done by expressing the reaction rate and the local generation rate as a function of the applied potential perturbation. At this point, distinction must be made between metal and semiconductor electrodes because of their different response to a change in electrode potential.

2.2. Metal Electrodes. Consider a single-step 1 equiv heterogeneous charge-transfer reaction



Let the rates of both reduction and oxidation be of first order in the electroactive species. The Butler–Volmer formulation of the electrode kinetics will then describe the behavior of this system in contact with a metal electrode as a function of the applied potential:¹¹

$$R_c = k_c c_{\text{Ox}}(0) = k^0 \exp[-\alpha(V - E^0)e/kT] c_{\text{Ox}}(0)$$

$$R_a = k_a c_{\text{Red}}(0) = k^0 \exp[(1 - \alpha)(V - E^0)e/kT] c_{\text{Red}}(0) \quad (8)$$

In these equations, R_c and R_a are the rate of the cathodic and the anodic half-reaction respectively; k^0 is defined as the conditional rate constant of the electrode reaction, i.e. the cathodic and anodic rate constant at equilibrium at the formal electrode potential E^0 . Finally, V stands for the potential applied to the working electrode.

A small-signal approximation expresses the dependence of these reaction rates on the variation of the applied potential and of the concentration of species near the interface:

$$\tilde{R}_c = k_c \tilde{c}_{\text{Ox}}(0) - \alpha \frac{e}{kT} k_c c_{\text{Ox}}(0) \tilde{V}$$

$$\tilde{R}_a = k_a \tilde{c}_{\text{Red}}(0) + (1 - \alpha) \frac{e}{kT} k_a c_{\text{Red}}(0) \tilde{V} \quad (9)$$

In this case, the electrochemical impedance equals the ratio of the variation of the applied potential to the total current⁹ (the cathodic current is conventionally defined as being negative):

$$Z = \frac{\tilde{V}}{e(\tilde{R}_a - \tilde{R}_c)} \quad (10)$$

The combination of (6), (9), and (10), together with the consideration that the local generation rate of the oxidizing agent equals the reaction rate of the reducing agent and vice versa, yields indeed the equations for the Randles circuit as proposed by Macdonald et al.⁹

This short example illustrates well the procedure followed. By means of a kinetic model, one is able to couple the mass transport as expressed in (6) to the variation of the applied potential. This results in an expression for the electrochemical impedance, which applies to those systems obeying the particular kinetics assumed.

2.3. The Semiconductor/Electrolyte Contact. The kinetics of an electrode process involving a semiconductor biased in the depletion range differs markedly from the kinetics at a metal electrode. A potential variation applied to an ideal semiconductor/electrolyte interface under depletion conditions will result in an equal change in the potential drop across the space-charge layer in the semiconductor. Thus the energy bands of the semiconductor are pinned at its surface, so that the rate constants of a reaction like (7) are potential-independent.⁷ However, the densities of the free charge carriers in the respective energy bands at the surface of the semiconductor are modified if the potential drop across the depletion layer changes. This causes the rates of the reactions in which these charge carriers are directly involved (capture processes) to be potential-dependent.^{4,6} On the other hand, the rate of an injection process at an ideal semiconductor/electrolyte interface is not influenced by a potential variation.^{4,6} As may be expected from (6), this difference is reflected in the presence or absence of a diffusion component in the electrochemical impedance if, in the case of the injection process, the reverse reaction may be neglected.

On the contrary, at a nonideal semiconductor/electrolyte interface, the energy bands are not pinned at the semiconductor surface. This creates the possibility to modulate the injection rate by a potential variation,⁷ causing a diffusion impedance to appear in the electrochemical impedance for an injection process with a negligible reverse reaction as well.

As a general remark, it should be mentioned that the derivations presented in the following sections are all specified for cathodic reactions. A general treatment is given in Appendix B, showing that the reasoning is valid for anodic reactions as well. At semiconductor electrodes, however, experimental verification is much easier for cathodic reactions.

2.3.1. Capture Processes at Ideal Semiconductor/Electrolyte Contacts (Taking Electron Capture at n-type Semiconductors as an Example). The reaction rate of a 1 equiv single-step electron-capture process by an oxidizing agent in solution is proportional to the density of electrons at the semiconductor surface and to the concentration of oxidizing species at the interface

$$R_c = k_c n_s c_{\text{Ox}}(0) \quad (11)$$

the rate constant k_c (and k_a , cf. *infra*) being determined by the overlap between the electronic energy levels in solution and the semiconductor energy bands.⁶ As mentioned before, k_c is

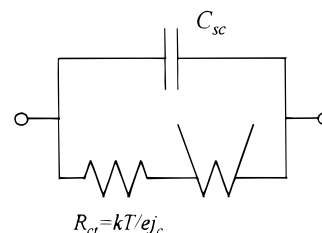


Figure 3. Randles-like equivalent circuit, calculated for capture processes at semiconductor electrodes. The Warburg impedance shown is an approximation of the diffusion impedance; C_{sc} is the capacitance of the depletion layer of the semiconductor.

independent of the applied potential for an ideal semiconductor/electrolyte contact. The rate of the reverse reaction (electron injection) is proportional only to the concentration of reducing species at the interface:⁶

$$R_a = k_a c_{\text{Red}}(0) \quad (12)$$

As shown in Appendix B, these rate equations allow us to calculate the impedance of this cathodic one-step capture process as ((b10), with the appropriate substitutions)

$$Z(\omega) = \frac{kT}{e(|j_c| + ek_a c_{\text{Red}}(0))} + \frac{kT}{e^2} \frac{k_c n_s + k_a}{k_c c_{\text{Ox}}(0) n_s d(\omega)} \quad (13)$$

Here, $|j_c|$ stands for the absolute value of the net (cathodic) electrical current density. The impedance consists of a charge-transfer resistance in series with the diffusion impedance. It is interesting to consider, for both elements, the limits for either no reverse reaction ($k_a = 0$) or a significant reverse reaction rate ($ek_a c_{\text{Red}}(0) \gg |j_c|$). The diffusion component will be present in the impedance described by (13), regardless of the rate of the reverse reaction. On the contrary, the charge-transfer resistance amounts to $kT/e|j_c|$ if no reverse reaction occurs, whereas it becomes much smaller than this value and eventually vanishes if the rate of the reverse reaction becomes larger than the net electrical current density. The expression $kT/e|j_c|$ for the charge-transfer resistance is typical for a reaction step with a rate proportional to the density of conduction band electrons at the semiconductor surface.¹²

As mentioned already, an applied potential perturbation changes the potential drop across the space-charge layer of the ideal semiconductor electrode only. Hence, to obtain the impedance of the ideal interface, the impedance expressed by (13) should be placed in parallel with a capacitance representing the space-charge layer of the semiconductor.¹³ This results in a Randles-like equivalent circuit (Figure 3), the physical interpretation of the capacitance being different, however, from that in the circuit used to describe metal electrodes.

The impedance of electrode reactions at nonideal semiconductor/electrolyte contacts will be more complicated. It is, however, clear that modulation of the concentration of electroactive species at the interface will generally still be possible. Thus the presence of the diffusion impedance will be the rule at nonideal contacts as well.

2.3.2. Injection Processes at Ideal Semiconductor/Electrolyte Contacts (Taking Hole Injection at p-type Semiconductors as an Example). Direct hole injection at an ideal p-type semiconductor/electrolyte contact by a 1 equiv oxidizing agent in solution has a rate proportional to the concentration of the species at the interface:^{6,14}

$$R_c = k_c c_{\text{Ox}}(0) \quad (14)$$

The rate of the reverse reaction (hole capture) is proportional

to the density of valence band holes at the semiconductor surface:⁶

$$R_a = k_a p_s c_{\text{Red}}(0) \quad (15)$$

The calculations of Appendix B apply equally well to this case, yielding the following expression for the impedance of the injection process ((b9), with the appropriate substitutions):

$$Z(\omega) = \frac{kT}{e^2 k_a p_s c_{\text{Red}}(0)} + \frac{kT}{e^2} \frac{k_c + k_a p_s}{k_a c_{\text{Red}}(0) p_s d(\omega)} \quad (16)$$

The impedance again consists of a series connection of a charge-transfer resistance and the diffusion impedance. However, in the limit $k_a p_s = 0$ (no reverse reaction), it becomes infinite, hence no diffusion impedance will appear in the electrochemical impedance.

The reason for this is easily understood when combining the injection rate (14) with (6), assuming the local generation rate to be zero. This results in

$$\tilde{c}_{\text{Ox}}(0) = 0 \quad (17)$$

As we argued before, (17) means that no coupling exists between an applied potential perturbation and the mass transport to the electrode for an injection process if the counter reaction is not significant. By consequence, no diffusion impedance will appear in the electrochemical impedance spectra. For the direct injection process considered here, (17) results in an impedance $Z(\omega) = \infty$ (combining the equality $j_c = -e\tilde{R}_c$ with (14) and (17) yields $\tilde{j}_c = 0$ hence $Z(\omega) = \infty$).

For hole-injection processes at n-type semiconductors, (17) is equally valid (hence no diffusion impedance if the reverse reaction may be neglected) but the impedance as a whole will be finite due to the recombination process.^{15,16}

2.3.3. Injection Processes at Nonideal Semiconductor/Electrolyte Contacts. At a nonideal semiconductor/electrolyte contact, a variation of the electrode potential will result in a change of the potential drop across both the depletion layer of the semiconductor and the Helmholtz layer. This makes the rate constant for injection sensitive to an applied potential perturbation. Thus the small-signal equivalent of (14) should now be written as

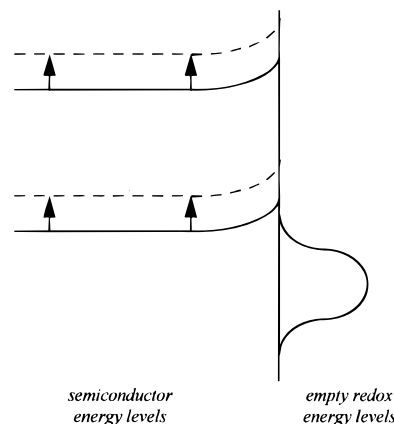
$$\tilde{R}_c = k_c \tilde{c}_{\text{Ox}}(0) + c_{\text{Ox}}(0) \tilde{k}_c \quad (18)$$

To proceed further, we will suppose \tilde{k}_c to be proportional to the applied voltage variation, hence $\tilde{k}_c = \kappa \tilde{V}$. Generally, the proportionality constant κ will be a complex, frequency-dependent quantity, determined by the particular mechanism governing the potential distribution across both the depletion layer and the Helmholtz layer.¹⁷ Inserting (18) into (6) yields an expression for the variation $\tilde{c}_{\text{Ox}}(0)$ as a function of the potential variation \tilde{V} :

$$\tilde{c}(0) = -\frac{\kappa}{k_c + d(\omega)} \tilde{V} \quad (19)$$

This equation indicates that, if the rate constant does not change when the electrode potential is varied ($\kappa = 0$),¹⁸ the modulation of the concentration near the interface will be zero. Thus, the mass transport will be independent of an applied potential variation, which means that no diffusion impedance will appear in the electrochemical impedance. On the other hand, the modulation of the concentration will be considerable if the rate constant is very sensitive to a changing electrode

good overlap
semiconductor/empty levels in solution



poor overlap
semiconductor/empty levels in solution

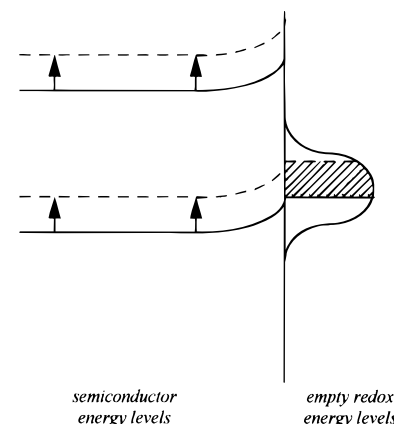


Figure 4. Effect of the overlap between valence band and empty energy levels in solution on the variation of the hole-injection rate constant, caused by unpinning of the band edges (depicted shift from solid to dashed line, shaded area representing additional overlap).

potential. In this case, the mass transport will be effectively coupled to the applied potential, thus introducing the diffusion component in the electrochemical impedance of the injection process as well.

For 1 equiv hole-injection reactions, the rate constant is associated with the overlap between the distribution function of the electronic states of the oxidizing agent and the valence band of the semiconductor.⁶ Figure 4 shows that, if this overlap is almost complete, a change of the energetic position of the valence band edge will not change this injection rate constant, hence $|\kappa| = 0$. If on the other hand the overlap is poor, unpinning of the valence band edge may change the injection rate constant considerably.

2.3.4. Multistep Reactions at Semiconductor/Electrolyte Contacts. The simple kinetic models used so far are not valid when dealing with a multistep reaction. To include the mass transport in the electrochemical impedance, an appropriate model of the electrode process is needed. This should provide an expression for the reaction rate R as a function of the applied potential and the concentration of active species at the interface, which can subsequently be used to calculate the whole impedance.

This relation will be more complicated than the ones used here for single-step reactions. Nevertheless, the principle expressed by (6) remains the same: if no modulation of the

concentration of active species at the interface is possible, the mass transport will not be coupled to the applied potential variation.

These considerations apply to 1 equiv hole-injection processes at n-type semiconductors, which are at least two-step reactions since the injection is systematically followed by electron-hole recombination. If the hole-injection rate is potential-independent, still no diffusion impedance will appear in the electrochemical impedance of these systems.

3. Experimental Section

All electrodes used were (100) faces of single-crystal semiconductors, obtained from MCP Electronics. The n-GaAs, n-InP and p-InP electrodes were doped with Si ($2.3 \times 10^{16} \text{ cm}^{-3}$), Sn ($6.7 \times 10^{17} \text{ cm}^{-3}$), and Zn ($7.8 \times 10^{16} \text{ cm}^{-3}$), respectively. They were all mounted as disk electrodes with a diameter of 4 mm.

The solutions were prepared using reagent grade chemicals, except for the methylviologen dichloride, which was 98% pure. The pretreatment of the electrodes consisted of mechanical polishing, followed by a dip in 12 M HCl for InP or a short etch in a mixture of H_2SO_4 (98%)– H_2O_2 (30%)– H_2O (3:1:1) for GaAs.

The experiments were carried out in a conventional three-electrode electrochemical cell using a saturated calomel electrode (SCE) as the reference electrode. The electrochemical impedance was always measured under potentiostatic control, using a potentiostat (EG&G, model 273) and a frequency-response analyzer (Solartron 1250). The amplitude of the small-signal perturbation (rms) varied, depending on the noise level, between 10 and 20 mV.

4. Experimental Results

4.1. Electron Capture: n-GaAs/ MV^{2+} . As reported by Schoenmakers et al.,¹⁹ methylviologen, dissolved as MV^{2+} , is reduced by electron capture at the n-CdS electrode. Furthermore, these authors showed that in a H_2O – $\text{C}_2\text{H}_5\text{OH}$ (1:1) mixture, the final reaction product MV^0 is not absorbed at the CdS surface, in contrast to the behavior in aqueous solutions.

In a cyclic voltammogram registered at n-GaAs in a mixture of equal volumes H_2O and $\text{C}_2\text{H}_5\text{OH}$, MV^{2+} shows two separate reduction waves in the forward scan whereas no reoxidation is observed during the reverse scan.¹² These waves correspond to the reduction of MV^{2+} to $\text{MV}^{+\bullet}$ and to MV^0 respectively. Considering the low E^0 potential of the $\text{MV}^{2+}/\text{MV}^{+\bullet}$ couple ($\approx -680 \text{ mV}$ vs SCE) and the position of the flat-band potential of n-GaAs in the H_2O – $\text{C}_2\text{H}_5\text{OH}$ mixture ($\approx -1300 \text{ mV}$ vs SCE), electron capture can be considered to be the probable reaction mechanism for the reduction of MV^{2+} at n-GaAs as well.

Figure 5 shows an electrochemical impedance spectrum, measured at a fresh n-GaAs surface in the current plateau of the MV^{2+} to $\text{MV}^{+\bullet}$ reduction. The capacitive semicircle at high frequencies and the Warburg impedance (line with slope -1 in the Nyquist plane) at low frequencies correspond fairly well to the calculated impedance, (13), for direct electron capture. Moreover, the dependence of the charge-transfer resistance on the absolute value of the cathodic current¹² supports the assumption that the reverse reaction is negligible (see (13)). This conclusion is consistent with the cyclic voltammetric results.

It must be mentioned that after the electrode has been kept in the reduction plateau for a few minutes, the impedance spectrum changes. The first semicircle is then followed by a second one, which passes into a Warburg impedance at low frequencies. This may point to a slowly initiated charge transfer

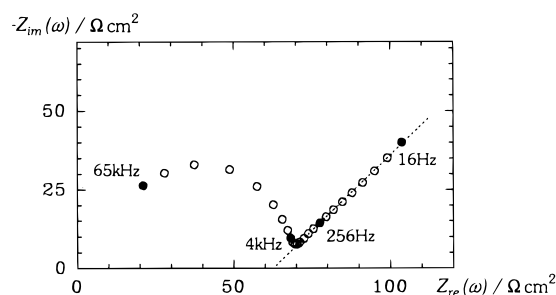


Figure 5. Nyquist representation of the impedance spectrum measured at n-GaAs/ MV^{2+} , using a fresh GaAs electrode: rotating disc electrode ($f_{\text{rot}} = 10 \text{ Hz}$), 2.2 mM MV^{2+} in H_2O – $\text{C}_2\text{H}_5\text{OH}$ mixture, $V = -1050 \text{ mV}$ vs SCE. The slope of fitting line was 0.96.

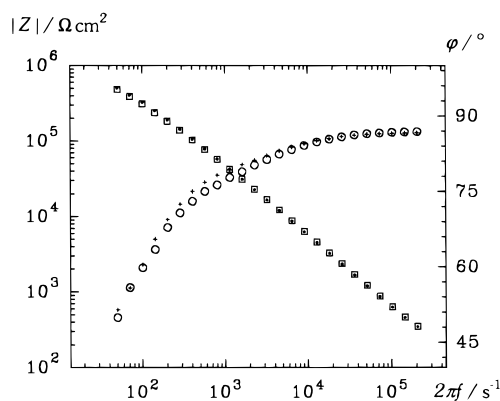


Figure 6. Bode representation of the impedance spectra measured at p-InP (rotating disc electrode, $f_{\text{rot}} = 10 \text{ Hz}$): amplitude and phase angle in aqueous KOH, $\text{pH} \approx 14$ (* and +) and with 0.5 mM $\text{Fe}(\text{CN})_6^{3-}$ added to solution (\square and \circ), $V = -600 \text{ mV}$ vs SCE.

through surface states, possibly in accordance to the behavior of MV^{2+} at p-GaAs.¹² Further research of this phenomenon was, however, beyond the scope of this paper.

4.2. Hole Injection at Ideal Semiconductor/Electrolyte Contacts: p-InP/ $\text{Fe}(\text{CN})_6^{3-}$ ($\text{pH} \approx 14$). The InP/ $\text{Fe}(\text{CN})_6^{3-}$ system at $\text{pH} \approx 14$ was studied by Vermeir et al.²⁰ They showed that the reduction of $\text{Fe}(\text{CN})_6^{3-}$ to $\text{Fe}(\text{CN})_6^{4-}$ at p-InP in alkaline solutions is a hole-injection process. A current density vs potential curve, measured at a rotating disc electrode, reveals indeed a diffusion-limited reduction plateau under cathodic polarization.

The band bending is large at the potential we used for electrochemical impedance spectroscopy at this system ($V - V_{\text{fb}} = 650 \text{ mV}$). Since the material used is not highly doped ($N_{\text{A}} = 7.8 \times 10^{16} \text{ cm}^{-3}$), this implies that the capacitance of the depletion layer is very small compared to that of the Helmholtz layer. Moreover, plotting C_{p}^{-2} vs V obtained from Mott–Schottky measurements yielded a straight line when the semiconductor was biased under depletion conditions. The combination of both arguments indicates (but does not prove²¹) that this contact may be considered as ideal under the experimental conditions.

Figure 6 shows the electrochemical impedance spectrum of p-InP both in indifferent electrolyte (KOH, $\text{pH} \approx 14$) and with $\text{Fe}(\text{CN})_6^{3-}$ added to solution, measured in the reduction plateau ($V = -600 \text{ mV}$ vs SCE). For better separation of the data at different frequencies, the Bode representation is preferred here. The electrochemical impedance itself is not affected at all by the $\text{Fe}(\text{CN})_6^{3-}$ in solution, i.e. no coupling exists between the mass transport to the interface and a change in applied potential, as expected at an ideal contact. Furthermore, this confirms that the reverse reaction is insignificant at this system, in accordance to the large band bending applied.

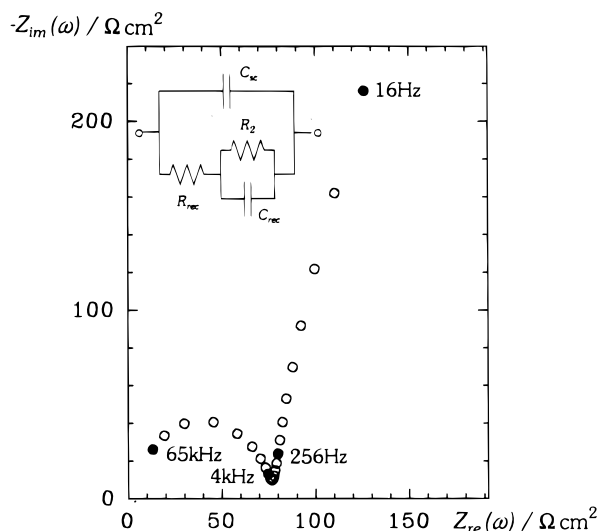


Figure 7. Nyquist representation of the impedance spectrum obtained at n-GaAs/Ce⁴⁺ in 1M H₂SO₄ aqueous solution: rotating disc electrode ($f_{\text{rot}} = 10$ Hz), 1.4 mM Ce⁴⁺, $V = -600$ mV vs SCE.

4.3. Hole Injection at Nonideal Semiconductor/Electrolyte Contacts: n-GaAs/Ce⁴⁺ (pH ≈ 0) and n-InP/Fe(CN)₆³⁻ (pH ≈ 14). A number of reasons renders the ideality of n-type semiconductor/electrolyte contacts with a hole-injecting agent in solution uncertain. The cathodic reduction plateau is generally relatively close to the flat-band potential. Moreover, due to electroless etching, the two systems under investigation show a shift of the band edges when going from anodic polarization (etching, no current flow) to cathodic polarization (no etching, current flow).^{20,22}

The Ce⁴⁺ ion dissolved in a 1 M solution of H₂SO₄ is a well-known hole-injecting oxidizing agent at GaAs.^{23,24} Because of the very high E^0 potential of the Ce⁴⁺/Ce³⁺ couple, the overlap between the electronic energy levels in solution and the valence band of the semiconductor is almost complete. However, the ideality of the n-GaAs/Ce⁴⁺ system is doubtful. In addition to the arguments mentioned, Mott–Schottky plots do not yield straight lines at bias potentials in the reduction plateau. In Figure 7, the impedance spectrum of the system n-GaAs/Ce⁴⁺ is shown, measured in the reduction plateau at -600 mV vs SCE. It may be approximately described by the electrical circuit shown in the inset of Figure 7, which consists of the recombination impedance¹⁵ in parallel with the capacitance of the depletion layer of the semiconductor. Apparently, no Warburg component is present in the electrochemical impedance of the system. This indicates that there is probably no coupling between the mass transport and the electrode potential.²⁵

In alkaline solutions (aqueous KOH, pH ≈ 14), Fe(CN)₆³⁻ is also reduced by hole injection at n-InP; however, in contrast with the n-GaAs/Ce⁴⁺ system, the rate of this reaction depends strongly on polarization. Measurements at rotating ring–disk electrodes show that the consumption of Fe(CN)₆³⁻ is kinetically controlled in the anodic polarization range and controlled by diffusion in the cathodic polarization range.²⁰ Clearly, the n-InP/Fe(CN)₆³⁻ system is not ideal in the transition region between both polarization ranges and, as Mott–Schottky measurements suggest, probably neither in the cathodic polarization range.²⁶

The impedance spectrum of this system is shown in Figure 8 (○). It consists of a flattened capacitive semicircle at high frequencies followed by a Warburg-like impedance at low frequencies. After subtraction of the high-frequency semicircle (approximated as a constant phase element $\sigma(i\omega)^{-\alpha}$ with $\alpha =$

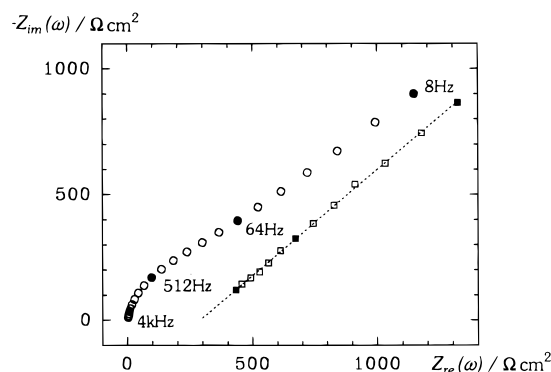


Figure 8. Nyquist representation of the impedance spectrum obtained at n-InP (rotating disc electrode, $f_{\text{rot}} = 10$ Hz): aqueous KOH (pH ≈ 14), 10 mM Fe(CN)₆³⁻, $V = -1200$ mV vs SCE (○). Spectrum with the high-frequency part subtracted is the line with slope 0.86 (□).

TABLE 1: Summary of the Coupling of Mass Transport to an Applied Voltage Perturbation for the (Cathodic) Reaction Types Discussed

	ideal semiconductor/ electrolyte contact	nonideal semiconductor/ electrolyte contact
electron capture (n-type)	yes	yes
hole injection (n- and p-type)	no	possible

0.94, in parallel to a resistance), the low-frequency part (Figure 8, □) has the shape of a straight line with a slope equal to 0.86, i.e. relatively close to the theoretically expected slope of a Warburg impedance.

Finally, it should be mentioned that the resistance in parallel to the constant phase element constituting the flattened semicircle at high frequencies is approximately 50 times larger than the value expected for the recombination resistance.^{15,16} For the time being, we have no explanation for this strong deviation.

5. Discussion and Conclusions

We showed that mass transport will only be coupled to an applied potential variation if this variation influences the concentration of electroactive species near the electrode/electrolyte interface. This condition is fulfilled, e.g. if a changing potential drop across the Helmholtz-layer affects the rate constants of the electrode reaction, as is generally the case at metal electrodes. At semiconductor electrodes, distinction must be made between capture and injection processes. Whereas a diffusion impedance should appear in the electrochemical impedance of a capture process, it will not in the case of an injection process at an ideal semiconductor/electrolyte contact if the reverse reaction is negligible (sections 2.3.1. and 2.3.2.). At nonideal semiconductor contacts, a shift of the band edge position may reflect itself in a diffusion impedance appearing in the electrochemical impedance spectra of an injection process (section 2.3.3.). Taking hole injection as an example, this will be the case if the shift of the valence band edge changes the overlap between the relevant energy levels in solution and the valence band considerably. Table 1 summarizes these ideas.

The experimental results presented show indeed that the diffusion impedance provides a straightforward way to discriminate between different kinds of processes. The clear distinction made between injection and capture processes at semiconductor electrodes by electrochemical impedance spectroscopy might be important, for instance, in the cathodic reduction of oxidizing agents at n-type semiconductors, in the case that no p-type is available (II–VI semiconductors) or that

the band edge position of n- and p-type electrodes is different so that the charge-transfer mechanism at n-type electrodes cannot be deduced from measurements at p-type electrodes.

In the case of hole injection at nonideal semiconductor/electrolyte contacts, the diffusion impedance may be of use to detect unpinning of the band edges. A crucial point here is whether this shift of the band edges has an appreciable influence on the rate constant for hole injection. At the n-InP/Fe(CN)₆³⁻ system, this is definitely the case. Only at cathodic potentials is the hole-injection rate diffusion-limited for this system, as demonstrated by Vermeir et al.²⁰ By consequence, a Warburg impedance should indeed be present in the electrochemical impedance of this system. In contrast, the hole-injection rate of Ce⁴⁺ at n-GaAs is both anodically and cathodically diffusion-limited, indicating that the dependence of this rate on the applied potential is negligible. Thus, no matter the ideality or nonideality of this contact, there should be no coupling between mass transport and applied voltage variation at this system, hence no Warburg impedance. This seems²⁶ to agree with the results obtained. Furthermore, as explained in section 2.3.3., the difference between both systems may be associated with the value of the E⁰ potential of the respective redox couples. The E⁰-potential of Ce⁴⁺/Ce³⁺ corresponds to a redox Fermi level approximately 0.5 eV below the valence band edge of n-GaAs in 1 M H₂SO₄²³ whereas for the Fe(CN)₆³⁻/Fe(CN)₆⁴⁻ couple, the E⁰ potential implies a position close to the valence band edge of n-InP in aqueous KOH at pH ≈ 14.²⁷

Acknowledgment. This work was performed within the framework of a G. O. A. (Gemeenschappelijk Overlegde Actie), financed by the Ministry of the Flemish Community (Belgium).

Appendix A: Solving Fick's Second Law

The diffusion of species between the bulk of the electrolyte and the electrode/electrolyte interface is modeled by the well-known diffusion equation.²⁸

$$\frac{\partial c(x,t)}{\partial t} = D \frac{\partial^2 c(x,t)}{\partial x^2} \quad (\text{a1})$$

Considering a steady state bias and a small-signal perturbation allows us to write this equation for the perturbation separately, using the appropriate boundary conditions. For a sinusoidal perturbation with frequency $\omega/2\pi$, the expression $\tilde{c}(x) \exp(i\omega t)$ may be used to solve (a1). This yields

$$i\omega \tilde{c}(x,\omega) = D \frac{d^2 \tilde{c}(x,\omega)}{dx^2} \quad (\text{a2})$$

Furthermore, the variation of the concentration should be zero at distances further from the interface than the diffusion layer thickness. This yields the boundary condition

$$\tilde{c}(\delta) = 0 \quad (\text{a3})$$

A general solution of this equation is

$$\tilde{c}(x) = A \exp\left(\sqrt{\frac{i\omega}{D}} x\right) + B \exp\left(-\sqrt{\frac{i\omega}{D}} x\right) \quad (\text{a4})$$

Using the boundary condition, the parameters A and B may be written as a function of $\tilde{c}(0)$, yielding

$$A = \tilde{c}(0) \exp\left(-\sqrt{\frac{i\omega}{D}} \delta\right) \left[\exp\left(-\sqrt{\frac{i\omega}{D}} \delta\right) - \exp\left(\sqrt{\frac{i\omega}{D}} \delta\right) \right]$$

$$B = -\tilde{c}(0) \exp\left(\sqrt{\frac{i\omega}{D}} \delta\right) \left[\exp\left(-\sqrt{\frac{i\omega}{D}} \delta\right) - \exp\left(\sqrt{\frac{i\omega}{D}} \delta\right) \right] \quad (\text{a5})$$

This allows us to calculate the diffusion current at the interface as

$$\tilde{j}|_{x=0} = -D \frac{d\tilde{c}}{dx}|_{x=0} = \sqrt{i\omega D} \coth\left(\sqrt{\frac{i\omega}{D}} \delta\right) \tilde{c}(0) = d(\omega) \tilde{c}(0) \quad (\text{a6})$$

Equation a6 implies a definition of the diffusion impedance $d(\omega)$. It is interesting to study this impedance considering the following limits

$$\lim_{\omega \rightarrow \infty} d(\omega) = \sqrt{i\omega D}$$

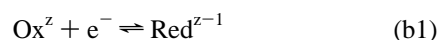
$$\lim_{\omega \rightarrow 0} d(\omega) = D/\delta \quad (\text{a7})$$

The inverse of the first limit yields the well-known Warburg impedance. The second means that if the frequency of the perturbation is low enough, the linear concentration profile over the diffusion layer is maintained.

Figure 2 shows a plot of $d(\omega)^{-1}$ in the Nyquist plane (negative imaginary axis upward), calculated assuming $D = \delta = 1$. As known, a Warburg impedance is depicted as a line with a slope equal to 1 in this representation. This is clearly the high-frequency limit of the impedance depicted. The figure shows moreover that deviations will occur if $(\omega/D)^{1/2} \delta \approx 1$. Taking $D = 10^{-5} \text{ cm}^2 \text{ s}^{-1}$, $\nu = 10^{-2} \text{ cm}^2 \text{ s}^{-1}$ and $f_{\text{rot}} = 10 \text{ Hz}$ yields $\delta \approx 2 \times 10^{-3} \text{ cm}^2$ implying that the Warburg impedance becomes invalid as an approximation of the diffusion impedance for frequencies below 1 Hz.

Appendix B: The Impedance of a 1 equiv Direct Electron-Transfer Reaction at an Ideal Semiconductor/Electrolyte Contact

We consider the reaction



involving conduction band or valence band electrons. At an n-type semiconductor, this implies electron capture by the oxidizing agent and electron injection by the reducing agent in solutions, whereas at p-type, (b1) can be considered as, respectively, a hole injection and a hole capture process. For both semiconductor types, we may write the respective reaction rates as⁶

$$R_{\text{inj}} = k_{\text{inj}} c_{\text{inj}}(0)$$

$$R_{\text{capt}} = k_{\text{capt}} x_s c_{\text{capt}}(0) \quad (\text{b2})$$

In this formula, c_{inj} and c_{capt} stand for the concentration of electroactive species in solution, the injecting and capturing charge carriers, respectively. The quantity x_s equals the surface concentration of conduction band electrons (n_s) at n-type and of valence band holes (p_s) at p-type semiconductors.

The electrical current density associated with a direct reaction equals (cathodic currents are by convention considered as negative)

$$j = ae(k_{\text{inj}} c_{\text{inj}}(0) - k_{\text{capt}} x_s c_{\text{capt}}(0)) \quad (\text{b3})$$

with $a = 1$ for n-type and $a = -1$ for p-type semiconductors. Applying a small-signal perturbation, (b3) becomes in terms of the small-signal quantities

$$\tilde{j} = ae(k_{\text{inj}}\tilde{c}_{\text{inj}}(0) - k_{\text{capt}}x_s\tilde{c}_{\text{capt}}(0) - k_{\text{capt}}c_{\text{capt}}(0)\tilde{x}_s) \quad (\text{b4})$$

since the reaction rate constants are assumed potential-independent. Next, (6) provides additional equations for both $\tilde{c}_{\text{capt}}(0)$ and $\tilde{c}_{\text{inj}}(0)$.

$$\begin{aligned}\tilde{G}_{\text{inj}} &= \tilde{R}_{\text{inj}} + d_{\text{inj}}(\omega)\tilde{c}_{\text{inj}}(0) \\ \tilde{G}_{\text{capt}} &= \tilde{R}_{\text{capt}} + d_{\text{capt}}(\omega)\tilde{c}_{\text{capt}}(0)\end{aligned} \quad (\text{b5})$$

Considering that the generation rate of the injecting species equals the reaction rate of the capturing species and vice versa and assuming that the diffusion coefficients of both species are equal, (b2) and (b5) yield

$$\begin{aligned}\tilde{c}_{\text{inj}} &= -\tilde{c}_{\text{capt}}(0) \\ \tilde{c}_{\text{capt}} &= -\frac{k_{\text{capt}}c_{\text{capt}}(0)}{k_{\text{capt}}x_s + k_{\text{inj}} + d(\omega)}\tilde{x}_s\end{aligned} \quad (\text{b6})$$

Inserting (b6) into (b4), the small-signal variation of the electrical current density becomes

$$\tilde{j} = -ae\left(\frac{k_{\text{capt}}c_{\text{capt}}d(\omega)}{k_{\text{capt}}x_s + k_{\text{inj}} + d(\omega)}\right)\tilde{x}_s \quad (\text{b7})$$

Finally, using the equality $\tilde{x}_s = -ax_s(kT/e)\tilde{V}$,¹⁵ the variation of the electrical current density may be expressed as a function of the applied voltage perturbation as

$$\tilde{j} = \left(\frac{k_{\text{capt}}c_{\text{capt}}d(\omega)}{k_{\text{capt}}x_s + k_{\text{inj}} + d(\omega)}\right)\frac{e^2}{kT}x_s\tilde{V} \quad (\text{b8})$$

The impedance of this reaction type is now readily obtained as

$$Z = \frac{kT}{e^2} \frac{1}{k_{\text{capt}}c_{\text{capt}}x_s} + \frac{kT}{e^2} \frac{k_{\text{capt}}x_s + k_{\text{inj}}}{k_{\text{capt}}c_{\text{capt}}x_s d(\omega)} \quad (\text{b9})$$

Finally, using (b3) describing the steady state, the impedance may be rewritten for cathodic processes at n-type or anodic processes at p-type semiconductors as

$$Z = \frac{kT}{e} \frac{1}{|j| + ek_{\text{inj}}c_{\text{inj}}} + \frac{kT}{e^2} \frac{k_{\text{capt}}x_s + k_{\text{inj}}}{k_{\text{capt}}c_{\text{capt}}x_s d(\omega)} \quad (\text{b10})$$

References and Notes

(1) Generally, this transport is a combination of diffusion and migration, caused by the electric field present. However, when working with a large excess of indifferent electrolyte, the latter contribution may be neglected.² We will assume this condition to be always fulfilled.

- (2) Brett, C. M. A.; Brett, A. M. O. *Electrochemistry: principles, methods and applications*; Oxford University Press: Oxford, 1993.
- (3) Gerischer, H. Z. *Phys. Chem.* **1960**, 26, 325.
- (4) Morrison, S. R. *Electrochemistry at Semiconductor and Oxidized Metal Electrodes*; Plenum Press: New York, 1980.
- (5) Randles, J. E. B. *Discuss. Faraday. Soc.* **1947**, 1, 11.
- (6) Gerischer, H. *Physical Chemistry, an Advanced Treatise*; Electrochemistry Vol. IXA; Academic Press: New York, 1970.
- (7) Vanmaekelbergh, D. *Electrochim. Acta* **1997**, 42, 1121.
- (8) The density of charge carriers (electrons or holes) at the semiconductor surface is not included in these rate constants.
- (9) Macdonald, J. R., Ed.; *Impedance Spectroscopy, Emphasizing Solid Materials and Systems*; John Wiley & Sons: New York, 1987.
- (10) It is convenient in electrochemical impedance spectroscopy to draw the negative imaginary axis upward, hence a slope equal to 1 in this representation is in fact equal to -1.
- (11) Koryta, J.; Dvorak, J. *Principles of Electrochemistry*; John Wiley & Sons: New York, 1987.
- (12) Hens, Z.; Gomes, W. P. J. *Electroanal. Chem.*, in press.
- (13) It is important to notice that one should not give a spatial interpretation to the diffusion impedance, in the sense of a potential drop across the diffusion layer. The electrical impedance, (14), describes the charge-transfer process at the interface, with the relevant potential drop standing across the depletion layer (reversely biased semiconductor electrodes) or the Helmholtz layer (metal electrodes). The diffusion process is coupled to this voltage variation because species are consumed or created at the interface, not because of any varying potential drop across the diffusion layer.
- (14) It should be clear that the rate constants k_c and k_a used in this paragraph are different from the ones used in 2.3.1.
- (15) Vanmaekelbergh, D.; Cardon, F. *J. Phys. D: Appl. Phys.* **1986**, 19, 643.
- (16) Lincot, D.; Vedel, J. J. *Electroanal. Chem.* **1987**, 220, 179.
- (17) Vanmaekelbergh, D. *Electrochim. Acta* **1997**, 42, 1135.
- (18) Although mathematically correct, this condition is physically too strict. However, since the intention of this paragraph is merely qualitative, it is not possible to write down a physically meaningful inequality.
- (19) Schoenmakers, G. H.; Waagenaar, R.; Kelly, J. J. *Ber. Bunsenges. Phys. Chem.* **1996**, 100, 1169.
- (20) Vermeir, I. E.; Gomes, W. P. J. *Electroanal. Chem.* **1994**, 365, 59.
- (21) Degryse, R.; Gomes, W. P.; Cardon, F.; Vennik, J. *J. Electrochem. Soc.* **1975**, 122, 711.
- (22) Schröder, K.; Memming, R. *Ber. Bunsenges. Phys. Chem.* **1985**, 89, 385.
- (23) Decker, F.; Pettinger, B.; Gerischer, H. *J. Electrochem. Soc.* **1983**, 130, 1335.
- (24) Kelly, J. J.; Notten, P. H. L. *Electrochim. Acta* **1984**, 29, 589.
- (25) Some uncertainty remains about the nature of R_2 (cf. Figure 7). Theoretically, this resistance expresses the competition between recombination and electroless etching. In the current plateau this results in a resistance, which is very large as compared to the recombination resistance.¹⁵ Still, other explanations are possible for the resistance measured. First, it may express the Faradaic resistance measured in indifferent electrolyte. Next, it may be a large charge-transfer resistance in series with a diffusion impedance, indicating a very small dependence of the hole-injection rate on the applied potential. These hypotheses could not be verified experimentally, due to noise generated by the rotating disk electrode at lower frequencies.
- (26) There is no necessary connection between a diffusion-limited current plateau and the ideality of the electrode/electrolyte contact. Diffusion limitation is reached if the condition $c(0) \ll c(\text{bulk})$ is satisfied. An increase in the reaction rate constants upon changing the applied potential will cause a decrease of $c(0)$, keeping the condition $c(0) \ll c(\text{bulk})$ fulfilled. Hence a current plateau is observed, regardless of the ideality or nonideality of the contact.
- (27) Vermeir, I. E. Ph.D. Thesis, Universiteit Gent, Gent, Belgium, 1994.
- (28) Vetter, K. J. *Electrochemical Kinetics, Theoretical and Experimental Aspects*; Academic Press: New York, 1967.